Journal of Thermal Analysis and Calorimetry (2023) 148:13157–13174
https://doi.org/10.1007/s10973-023-12313-y

Seville history insight through their construction mortars

Jose L. Perez-Rodriguez[1] · Luis A. Perez-Maqueda[1] · Maria L. Franquelo[1] · Adrian Duran[2]

Received: 20 November 2022 / Accepted: 6 June 2023 / Published online: 1 July 2023

Abstract

Seville is intimately linked to its historic role and extensive cultural heritage. The city has been occupied by Romans, Arabs and Christians, who built important historical buildings. Roman (first–second centuries) and Arabic (eleventh century) buildings, medieval Shipyard (thirteenth century), San Isidoro and Santa Maria de las Cuevas monasteries (fifteenth century), Santa María de las Cuevas (fifteenth century modified in eighteenth century), El Salvador Church (eighteenth century), the Royal Ordnance building (eighteenth century) and Santa Angela de la Cruz convent (twentieth century) performed with lining mortars, and mortars used in building stones (City Hall and Marchena Gate), all of them located in Seville (Spain), have been studied. Ninety-four mortar samples (employed as structural, plaster, coating) originally used or applied in restoration processes have been collected to perform an archaeometry study. The ratio of CO_2 mass loss to hydraulic water (H_2O) mass loss, and the mineralogical characterization by X-ray diffraction has been used to compare the mortars used in the different historical periods. Mainly hydraulic mortars were widely used in all these studied monuments as most mortars showed CO_2/H_2O ratios within the 4–10 range. Moreover, the thermal analysis curves also showed a broad temperature range for the thermal decomposition of the carbonate fraction of the mortars.

Keywords Sevillian historical mortars · Thermal analysis · XRD · Technology of mortars

Introduction

Analysis of ancient mortars

In recent years, some scientific studies dealing with the characterization and properties of ancient mortars have been published to improve the knowledge on the manufacture and management of new-building mortars and, consequently, to imitate their use in the past. Mortars are complex materials, which are prepared following receipts described since antiquity [1, 2]. The chemical and mineralogical characterization of historical mortars can shed light on the origin of the materials and techniques used for their construction. This information is very valuable in conservation and restoration of ancient buildings. Thus, the analysis of ancient mortars should be used to design compatible repair mortars. The archaeometric study of mortars also discriminates the different construction phases and the differences among buildings and, accordingly, civilizations and historical periods. Several studies have been published comparing the production technology of mortars manufactured in different historical periods [3–7]. Moropoulou et al. studied the mortar technologies of historical mortars from the city of Rhodes [5]. Sitzia compared mortars from the Roman to Medieval period in the site of San Saturnino Basilica in Italy [3], and Artioli et al. studied the development of binders in ancient constructions before and after the Roman Empire period [4]. Recently, Vlase et al. [7] studied nonhydraulic mortars from different periods (first century BC—106 AD and Medieval centuries) in Transylvania. Historical evidences of the use of mortars during several periods have been described in the literature. Thus, it is known that lime mortars have been widely used as building materials in Egyptian, Greek, Roman, Arabic and Christian periods [7–17]. During the Middle Ages, the building techniques were modified from the Roman parameters, consisting in more hydraulic mortars as mentioned Milanesio et al. [16] and Calandra et al. [17] in mortars from

✉ Luis A. Perez-Maqueda
maqueda@cica.es

✉ Adrian Duran
adrianduran@unav.es

[1] Materials Science Institute, CSIC-University of Seville, Americo Vespucio 49, 41092 Seville, Spain

[2] Department of Chemistry, School of Sciences, University of Navarra, Irunlarrea 1, 31008 Pamplona, Spain

Italy. From the second half of the nineteenth century, natural cement, produced without hydraulic addition to the raw materials, was employed in Europe, mainly in buildings in Austria, Poland and Portugal [18].

Historical studies refer to the use of mortars for different applications: as plaster on internal and external walls [7, 10, 16, 18], supporting materials for wall paintings (fresco or secco techniques) [9, 19], as joint mortars of masonry structure [7, 17, 20] or isolating lining materials in cistern, walls, shafts, etc. [5, 7, 21].

There are many possible techniques to be used for the characterization of the artworks. Thermal analysis techniques and high-temperature X-ray diffraction are highlighted as very useful techniques for these studies since they provide a complete characterization of mortars used in historical buildings. Thermogravimetric analysis is very useful for the characterization of mortars since it provides information on temperature ranges and relative mass losses corresponding to the different components [5, 7, 19, 22–24]: Thus, adsorbed water (< 120 °C), water of hydrated salts (120–200 °C), chemically bound or hydraulic water (200–600 °C, as far as there are no other compounds that undergo mass loss in this temperature range such as Portland cement, and the loss of CO_2 due to decomposition of carbonates (> 600 °C). The ratio between the mass losses corresponding to CO_2 and hydraulic water (CO_2/H_2O) is of particular interest and gives an adequate comparative information on the hydraulic nature of the mortar [5, 19, 25]. In the last twenty years, X-ray powder diffraction methods have been extensively used for the characterization of different materials of archaeological, historical and artistic interest. Moreover, high-temperature X-ray diffraction has been used to characterize the different phases formed during the heating of mortars under in situ conditions, helping in the characterization of the different processes taking place during the thermal treatment [26].

Constructions from Seville

The authors of this work have carried out multiple studies to characterize the materials used in existing historic buildings and artworks in Seville using destructive and non-destructive experimental techniques [8–12, 19, 20, 26–34]. Seville originally an Iberian town, flourished during Roman period, where several buildings: theater, circus, store, etc., were built. Several Roman constructions from first BC to second AD centuries have been found in the archaeological excavations inside the Real Alcazar of Seville. On top of these Roman ruins, several buildings were constructed from the tenth century onwards (during *emiral*, *califal*, *taifa-abbadita*, *almoravide* and *almohade* stages). The extensive archaeological investigation carried out in the Alcazar of Seville has made possible to obtain remaining of these Roman and Arabic buildings [8–12]. After the conquest of Seville in 1248, Christians began to build Gothic and Mudejar palaces in the Alcazar of Seville. In the same period, many new constructions were also built [9, 28], such as the Shipyards, which are partially preserved today, constructed by the King Fernando III in the thirteenth century. In the fifteenth century, the Monasteries of San Isidoro del Campo (where Cistercians and Hieronymites monks lived) and Santa María de las Cuevas (Carthusian monks) were built. In the former, the ancient mortars were covered at that time with frescco wall paintings, while in the latter, the ancient mortars were covered with stucco paintings in the eighteenth century [19, 26, 27]. Marchena Door and City Hall were built in the fifteenth and sixteenth centuries, respectively [20, 30, 32, 34]. The Royal Ordnance was initially completed in the eighteenth century although some restoration processes were carried out later on [29]. The construction of El Salvador Church took place between 1674 and 1712 [19]. Finally, Santa Angela Convent was constituted in the nineteenth century. An accurate characterization improved the knowledge of the mortars from these historical monuments of the city of Seville, which also has allowed a comparison between them, and furthering the development of successful intervention techniques. The buildings rests found in excavations and the restoration treatments of monuments in Seville have facilitated sampling of both original mortars and materials used in recent restoration. This study has permitted to know the constitution and use of different mortars used in monuments of Seville and compare them from the various epochs.

The current research focuses on the archaeometric study of different mortars from Seville corresponding to different historical periods starting from Roman times up to the twentieth century, including Arabic, Mudejar and different Christian periods. This study allows to compare the production technology over the centuries. Moreover, a better knowledge on the manufacturing techniques and the application methods used in the past provides relevant information for restoration and conservation.

Materials and methods

Materials

Both Roman (AP_R) and Arabic (AP_A) mortars were obtained from the archaeological excavations in Patio de Banderas in the Real Alcazar Palace (AP) of Seville (Figs. 1a and 1b). Romans mortars were from the first–second centuries, while the Arabic are from the eleventh century. These mortars have not been restored and, therefore, they are in their original state. In total, ten Roman and six Arabic mortar samples were analyzed. Half of the samples (AP_R2i,

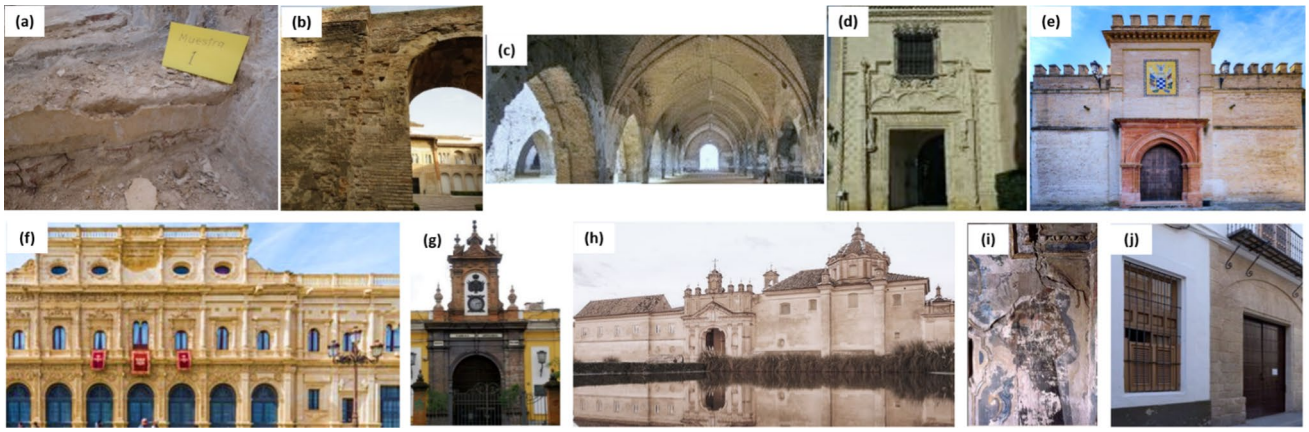

Fig. 1 Images of the monuments studied: (**a**,**b**) Roman and Arabic mortars from Reales Alcazares, **c** Shipyard building, **d** Marchena Door, **e** San Isidoro Monastery, **f** City Hall, **g** Royal Ordnance Factory, **h** Monastery of Santa Maria de las Cuevas, **i** Mortars from El Salvador Church, **j** Santa Angela Convent

AP_R3i, AP_R12i, AP_R14i, AP_R16i, AP_A1i, AP_A1bi and AP_A2i) were collected from the internal and the other half (AP_R3e, AP_R10e, AP_R12e, AP_R14e, AP_R16e, AP_A1e, AP_A1be and AP_A2e) from the external parts within the constructive walls (Table 1).

The Shipyard building (SH) was built in the thirteenth century, but has been transformed several times due to the different uses it has had over time. Although most walls were modified, the wall made of bricks and mortars (samples SH_M2, SH_M5, SH_M28 and SH_M30) was in its original state (Table 1, Fig. 1c).

Marchena Door (AP_M) was built in 1493 in Marchena city close to Seville. In 1913, the Door was moved into Seville Real Alcazar Palace garden (Fig. 1d). The monument has so far undergone few interventions. Six samples were collected for the study: four original (AP_M1, AP_M2, AP_M3 and AP_M4) and two corresponding to restorations (AP_MD1* and AP_MD2*) (all the samples with and asterisk corresponded to restoration mortars) (Table 1).

Regarding the samples from San Isidoro Monastery (SI) (Fig. 1e), they are original and in excellent conditions. Eight samples were studied (SI_M1, SI_M2, SI_M3, SI_M6, SI_M7, SI_M8, SI_M9 and SI_M14) (Table 1). The original fifteenth century ribbed vault was hidden with another barer vault performed in 1632.

The construction of the Seville City Hall (CH) building started in the sixteenth century. Seville City Hall is one of the more striking examples of the Plateresque architectural style in Andalusia (Fig. 1f). For the construction, a soft stone was selected since it could be easily carved. Multiple restoration processes were detected in this monument in different periods. Fifteen restoration mortar samples were collected and analyzed (CH_1*, CH_2*, CH_4*, CH_5*, CH_6*, CH_8*, CH_9*, CH_10*, CH_15*, CH_33*, CH_53*, CH_54*, CH_67*, CH_68* and CH_CM*).

The Royal Ordnance Factory of Seville (RO), constituted as the main example of industrial architecture in the city, was in use until the final of the twentieth century (Fig. 1g). Some constructive phases were developed along the eighteenth century. Original (RO_B, RO_C, RO_D, RO_F, RO_1Bl, RO_1Cl, RO_2 and RO_3) and restoration (RO_4Bl* and RO_4Cl*) mortars were collected for this study (Table 1).

In the case of the Monastery of Santa María de las Cuevas (Carthusian convent) (SM) (Fig. 1h), a large part of the walls was covered with stucco, whose main component was gypsum, on which the mural paintings were made. Most of these wall paintings dated from the eighteenth century (samples SM_Ae, SM_Ai, SM_D, SM_I, SM_Ke, SM_Ki, SM_Le, SM_Li, SM_Me, SM_Mi, SM_N) (Table 1). The presence of this stucco means that most of the mortars studied have plaster (SM_Ae, SM_Ke, SM_Le and SM_Me). In later times, a ceramic factory was set in this building, which may also be responsible for the contamination with sulfur. In the late 1980s and early 1990s, the building was recovered as a museum and, during this later time, the mortars were taken for the study.

El Salvador Church (ES) is a typical example of Sevillian Baroque construction. The studied samples were collected from columns of the main room (ES_CS1, ES_RSe and ES_RSi) (Table 1 and Fig. 1i). Integral restoration was completed in this Church in the period 2004–2010.

For Santa Angela convent (SA) (Fig. 1j), two groups of samples were considered: some originals (samples SA_2, SA_6, SA_10 and SA_12) from the end of the nineteenth or the beginning of the twentieth centuries when nuns arrived at the convent (1890), and others from a recent restoration from the beginning of the twenty-first century (samples SA_16*, SA_17* and SA18*) (Table 1).

Table 1 Mass losses and ratios from thermal studies, corresponding to all mortars

	< 120 °C	120–200 °C	200–600 °C (structural H_2O)	> 600 °C (CO_2)	Total loss mass (25–1000 °C)	CO_2/structural H_2O	%$CaCO_3$
■ ALCAZAR PALACE_ROMAN MORTARS (s. I–II)							
AP_R2i	0.38	0.11	1.24	6.85	8.58	5.52	15.57
AP_R3e	0.61	0.16	1.55	9.78	12,10	6.31	22.23
AP_R3i	0.58	0.16	1.65	11.32	13.71	6.86	25.73
AP_R10e	1.07	0.49	3.11	15.37	20.04	4.94	34.93
AP_R12i	0.40	0.10	1.53	10.91	12.94	7.13	24.80
AP_R12e	0.37	0.14	1.73	19.02	21.26	10.99	43.23
AP_R14i	0.42	0.15	1.63	9.93	12.13	6.09	22.57
AP_R14e	0.82	0.37	3.04	19.36	23.59	6.37	44.00
AP_R16i	0.34	0.13	1.46	8.70	10.63	5.96	19.77
AP_R16e	0.39	0.22	2.75	19.67	23.03	7.15	44.70
■ ALCAZAR PALACE_ARABIC MORTARS (s. XI)							
AP_A1i	0.82	0.32	2.63	14.34	18.11	5.45	32.59
AP_A1e	1.31	0.61	4.55	26.14	32.61	5.75	59.41
AP_A1bi	0.48	0.31	2.89	13.24	16.92	4.58	30.09
AP_A1be	1.16	0.64	5.36	26.68	33.84	4.98	60.64
AP_A2i	0.68	0.25	2.48	12.61	16.02	5.08	28.66
AP_A2e	1.15	0.53	4.50	23.65	29.83	5.26	53.75
■ SHIPYARD_MEDIEVAL (s. XIII)							
SH_M2	2.68	0.22	6.33	22.13	31.36	3.50	50.29
SH_M5	1.96	0.47	4.45	24.71	31.59	5.55	56.27
SH_M28	10.10	0.32	5.34	20.75	36.51	3.89	47.16
SH_M30	2.09	0.58	4.30	20.28	27.25	4.72	46.09
● ALCAZAR PALACE_MARCHENA DOOR (s. XV)							
AP_M1	2.00	0.45	4.65	26.84	33.94	5.77	61.00
AP_M2	2.68	0.33	4.35	25.96	33.32	5.95	59.01
AP_M3	–	–	–	–	–	–	–
AP_M4	–	–	–	–	–	–	–
AP_MD1*	0.72	0.23	2.21	26.61	29.77	12.04	60.48
AP_MD2*	0.74	0.24	1.57	24.57	27.12	15.65	55.84
● SAN ISIDORO (s. XV–XVI)							
SI_M1	1.36	0.71	3.66	24.28	30.01	6.63	55.18
SI_M2	–	–	–	–	–	–	–
SI_M3	–	–	–	–	–	–	–
SI_M6	–	–	–	–	–	–	–
SI_M7	–	–	–	–	–	–	–
SI_M8	1.22	0.70	3.74	29.4	35.06	7.86	66.82
SI_M9	–	–	–	–	–	–	–
SI_M14	1.49	0.79	4.55	23.25	30.08	5.11	52.84
● CITY HALL (s. XVI)							
CH_1*	0.69	0.70	6.34	12.88	20.61	2.03	29.27
CH_2*	–	–	–	–	–	–	–
CH_4*	0.71	0.50	3.24	17.31	21.76	5.34	39.34
CH_5*	1.13	1.02	3.81	19.40	25.36	5.09	44.09
CH_6*	1.61	16.05	1.50	4.60	23.76	3.07	10.45
CH_8*	0.58	18.76	0.82	2.19	22.35	2.67	4.98

Table 1 (continued)

	< 120 °C	120–200 °C	200–600 °C (structural H_2O)	> 600 °C (CO_2)	Total loss mass (25–1000 °C)	CO_2/structural H_2O	%$CaCO_3$
CH_9*	1.32	12.81	4.79	8.95	27.87	1.87	20.34
CH_10*	0.76	0.38	2.29	13.44	16.87	5.87	30.55
CH_15*	0.61	0.64	1.03	40.94	43.22	39.75	93.05
CH_33*	0.80	0.70	2.40	38.62	42.52	16.09	87.77
CH_53*	0.31	3.53	2.29	34.12	40.25	14.90	77.55
CH_54*	3.13	8.28	5.15	18.13	34.69	3.52	41.1.20
CH_67*	1.54	7.40	11.65	18.81	39.40	1.61	42.75
CH_68*	2.04	15.60	0.74	2.43	20.81	3.28	5.52
CH_CM*	1.64	0.59	2.86	4.87	9.96	1.70	11.07
▲ ROYAL ORDNANCE (s. XVIII)							
RO_B	3.00	8.40	3.46	19.57	34.43	5.66	44.48
RO_C	2.17	4.86	2.95	29.62	39.60	10.04	67.32
RO_D	1.55	1.50	4.34	26.93	34.32	6.21	61.20
RO_F	1.46	1.08	4.47	18.55	25.56	4.15	42.16
RO_1Bl	2.06	7.68	3.12	22.53	35.39	7.22	51.20
RO_1Cl	1.54	1.50	4.85	30.0.10	37.99	6.21	68.41
RO_2	–	–	–	–	–	–	–
RO_3	1.82	2.57	3.78	20.44	28.61	5.41	46.45
RO_4Bl*	0.05	0.42	2.15	41.22	43.84	19.17	93.68
RO_4Cl*	1.10	0.34	2.67	34.21	38.82	12.81	77.15
▲ SANTA MARIA_CUEVAS (s. XVIII)							
SM_Ae	0.08	9.85	1.43	2.81	14.17	1.97	6.39
SM_Ai	0.16	1.56	6.01	27.11	34.84	4.51	61.61
SM_D	0.09	1.25	5.48	24.92	31.74	4.55	56.64
SM_I	–	–	–	–	–	–	–
SM_Ke	0.09	9.28	1.39	4.59	15.40	3.30	10.43
SM_Ki	0.07	0.65	4.92	24.99	30.63	5.08	56.80
SM_Le	1.01	7.88	2.00	8.49	19.38	4.25	19.30
SM_Li	0.57	0.88	5.58	25.33	32.36	4.54	57.57
SM_Me	0.15	11.45	2.55	9.49	23.64	3.72	21.57
SM_Mi	0.44	1.01	5.21	26.52	33.18	5.09	60.27
SM_N	0.55	0.79	3.59	27.11	32.04	7.55	61.61
▲ EL SALVADOR (s. XVIII)							
ES_CS1	0.21	0.71	3.94	27.14	32.00	6.89	61.68
ES_RSe	0.08	7.56	6.01	17.56	31.21	2.92	39.91
ES_RSi	0.18	0.91	5.98	31.48	38.55	5.26	71.55
▲ SANTA ANGELA (s. XIX–XX)							
SA_2	0.16	0.03	1.55	26.31	28.05	16.97	59.80
SA_6	1.27	0.36	2.42	25.65	29.70	10.60	58.30
SA_10	0.48	0.02	1.30	24.86	26.66	19.12	26.50
SA_12	2.23	2.75	3.63	21.65	30.26	5.96	49.20
SA_16*	0.57	0.08	1.34	16.71	18.70	12.47	37.98
SA_17*	0.34	0.08	1.45	15.03	16.90	10.37	34.16
SA_18*	0.60	0.07	3.28	12.98	16.93	3.96	29.50

* Restoration mortars

Methods

The samples were collected from the mortar samples, dried in an oven at 40 °C during 24 h and crushed in an agate mortar. The mortar layer samples were analyzed together, so binder and aggregate were not differentiated and analyzed together. In the case of Shipyard samples, small pieces of bricks could be identified using a magnifying glass and eliminated from mortar samples by hand.

Simultaneous thermogravimetry–differential scanning calorimetry (TG-DSC) and thermogravimetry–differential thermal analysis (TG–DTA) measurements were performed by using STDQ600 TA Instruments and TG-sDTA 851 Mettler Toledo devices. Samples were measured between 25 and 1000 °C at a linear heating rate of 10 °C·min^{-1} in air flow. In some cases, CO_2 gas flow was used to investigate the possible presence of dolomite. The amount of organic matter was determined from the TG mass loss in the temperature range from 200 to 600 °C, when an exothermic effect in the DTA curve due to the combustion process was recorded.

X-ray diffraction (XRD) experiments were carried out using a Panalytical model X'Pert Pro MPD diffractometer. Data were collected in a 2Θ range of 3–60°, with step of 0.02° and 1 s step. Source was a Cu anode (Cu-Kα radiation), operating at 40 kV and 40 mA. Scintillator detectors were used. Diffractograms were collected every 50 °C in the temperature range from 25 to 1000 °C (heating rate 10 °C·min^{-1}). The methods for semiquantitative analyses are included in the software of the apparatus, based on the direct measurements of intensities of individual XRD reflections. This model uses RIR (Relative Intensity Ratio) data document for crystalline phases of unknown compounds in the ICDD (International Centre for Diffraction Data) PDF (Powder Diffraction File) database and 50/50 mixture of corundum. PDF reference cards have been cited for each crystalline phase.

Elemental analyses were performed by using X-ray fluorescence (XRF) and energy-dispersive X-ray spectroscopy (EDX). For the XRF analyses, a Bruker S2 Puma equipment with a silver anode and helium atmosphere was used. Samples were analyzed with a 4 µm polypropylene filter. Quantification was performed with the *Spectra Result Manager* software. An EDX Bruker-X Flash-4010 analyzer was coupled to the scanning electron microscopy (Hitachi S-4800).

FTIR analyses were done in a Shimadzu IR Affinity-1S spectrophotometer coupled with an attenuated total reflectance (ATR) accessory Golden Gate. Measurements were performed in the wavenumber range 4000–600 cm^{-1} with a resolution of 4 cm^{-1} and 100 scans by sample.

Results and discussion

The studied mortars from the different historic buildings of Seville were divided in two groups: the first one was constituted for masonry structures, lining layers coating the monuments or used as joining mortars, while the second one included plaster to cover the loss of materials and restoration materials (inorganic and organic) applied to stone buildings.

Thermogravimetric analysis was used for characterization of mortars, as it provides information about the amount of structural water and carbonates from the different relative mass losses. Results from thermogravimetric analysis for the different studied samples are depicted in Table 1. Moreover, Fig. 2 shows the ratio of CO_2 to structural H_2O versus $\%CO_2$, while Fig. 3 shows the %structural H_2O vs $\%CO_2$ for all the mortars. Additionally, X-ray diffraction analysis also provides relevant complementary information for the characterization of the different mortars as depicted in Table 2. Moreover, XRF and SEM–EDX elemental analyses were also performed to corroborate XRD data and FTIR-ATR for detecting the vibration modes of hydraulic and organic compounds.

Lining mortars

Fabrics mortars employed to cover the buildings.

Roman mortars (first–second centuries) (samples AP_R)

Two different groups of Roman mortars could be identified by thermogravimetric analysis (Table 1, Figs. 2 and 3). The first group of samples (AP_R2i, AP_R3i, AP_R12i, AP_R14i and AP_R16i), with lower percentage of calcium

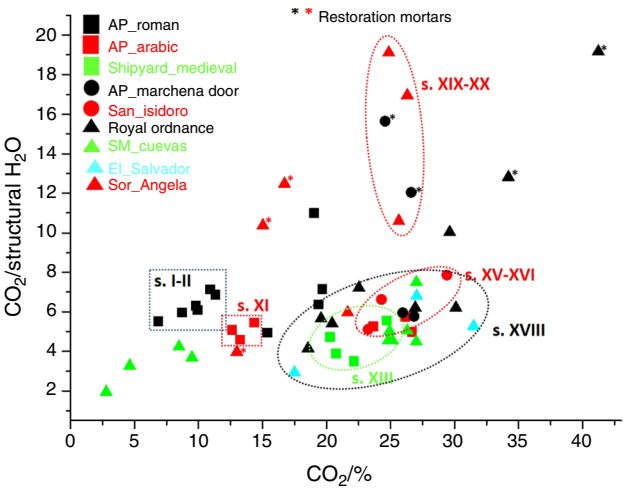

Fig. 2 Representation of CO_2/structural H_2O ratio vs $\%CO_2$ from all studied mortars (except those from City Hall)

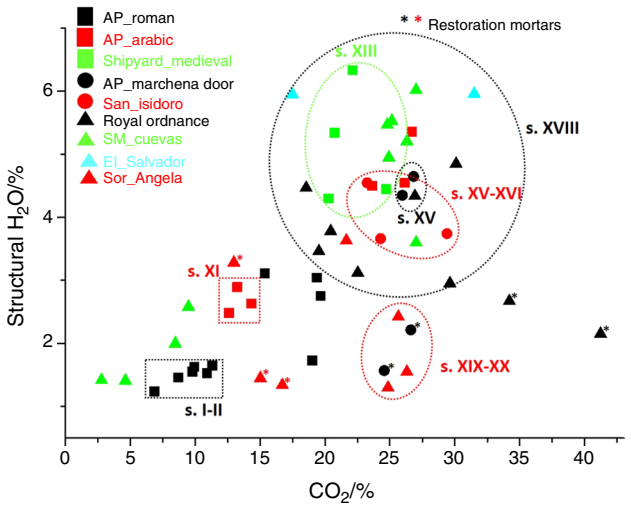

Fig. 3 Representation of %structural H_2O vs $\%CO_2$ for all the mortars (except those from City Hall)

carbonate, was attributed to inner layers of mortars that were covered with other layers belonging to the second group of samples (AP_R10e, AP_R12e, AP_R14e and AP_R16e), with higher calcium carbonate percentage, that corresponded to the layers located on the external surface of the walls. Moreover, the average ratio CO_2/H_2O was higher for the external (7.15) than for the internal (6.31) layers. As an example of the Roman mortars, Fig. 4a shows the TG and DTA curves corresponding to the sample AP_R14i. Two endothermic signals were observed: at ca. 573 °C, corresponding to the polymorphic α-β transformation in quartz, and at ca. 725 °C, corresponding to the thermal decomposition of calcium carbonate. The semiquantitative XRD analyses, based on the intensity of the reflections (Table 2), matched the results provided by the thermal analysis. Thus, calcite percentages of circa 25% were calculated for internal mortars and of 50% approximately for the external ones. In addition, significant amounts of quartz were also observed both for internal (70%) and external (40%) mortars, while dolomite was only detected for samples AP_R12e and AP_R16e (Table 2). XRD diffractogram of the sample AP_R14i (Fig. 5a) showed quartz (SiO_2, PDF 33–1161), calcite ($CaCO_3$, PDF 05–0586) and other minority feldspars phases such as anorthite ($CaAl_2Si_2O_8$, PDF 41–1486) and albite ($NaAlSi_3O_8$, PDF 01–0739). XRF analyses of sample AP_R14i corroborated the XRD and thermal analysis results, showing the presence of Si, Ca, Fe, Al and K (Table 3 and Supplementary Figure S1a).

Arabic mortars (eleventh century) (samples AP_A)

The thermal study of these samples also showed two groups of mortars (Table 1, Figs. 2 and 3) attributed to the presence of an internal layer of mortar (samples AP_A1i, AP_A1bi and AP_A2i) covered by others surface layers (samples AP_A1e, AP_A1be and AP_A2e), similarly to Roman mortars. As an example of the Arabic mortars, Fig. 4b shows the TG and DTA curves corresponding to the sample AP_A2i, showing similar thermal effects than the Romans. Semi-quantitative XRD results indicated calcite percentages of 30% and 60% for internal and external mortars, respectively, matching with the TG results. Dolomite was found in Arabic mortars AP_A1e and AP_A2e. Mineralogical phases found in the sample AP_A2i were quartz, calcite and anorthite, likewise to Roman samples, and albite (Fig. 5b). Si, Ca, Fe, Al and K were the elements identified by XRF (Table 3 and Supplementary Figure S1b).

Medieval Shipyard (thirteenth century) (samples SH)

The Roman and Arabic mortars were coating the walls, whereas the mortars used in the Medieval Shipyard were used to join bricks that made up the walls as visually observed. In Figs. 2 and 3, all samples collected from this monument were grouped in just one zone. The values of carbonate percentages in the four samples from the Shipyard (SH_M2, SH_M5, SH_M28 and SH_M30) were very similar (Table 1). The ratio CO_2/H_2O was minor for these Medieval samples (4.42) probably due to the high amount of structural water from the rests of bricks accompanying the mortars. The amount of structural H_2O was higher for the Shipyard than that for Roman or Arabic mortars, especially the sample SH_M2 (Fig. 3 and Fig. 4c). In addition, FTIR-ATR spectrum showed the presence of bands at 1796, 1405, 872 and 713 cm^{-1}, assigned to carbonate phases (calcite), at 1029 cm^{-1}, characteristic of the Si–O–Si vibration, and others signals between 1100 and 600 cm^{-1}, corresponding to silico-aluminate compounds [7]. The presence of hydraulic phases could be attributed to the reaction of lime and bricks as mentioned above (Fig. 6a). The amounts of calcium carbonate, as determined by XRD, were slightly larger than those obtained by thermogravimetry. Table 3 and Supplementary Figure S1c show the XRF spectrum of the sample SH_M2, showing the presence of Si, Ca, Al and Fe.

San Isidoro Monastery (fifteenth century) (samples SI)

Figures 2 and 3 show that the three studied samples (SI_M1, SI_M8 and SI_M14) were depicted in a narrow zone (Table 1). Figure 4d shows the thermal curves of the sample SI_M8 as an example from this monument and Fig. 6b the infrared spectrum which showed the presence of silicates at 1084 cm^{-1}. XRD analysis was extended to eight samples (SI_M1, SI_M2, SI_M3, SI_M6, SI_M7, SI_M8, SI_M9 and SI_M14). Two different groups were differentiated (Table 2): one constituted by samples with 70% of calcite and 20% of

Table 2 Crystalline phases from X-ray diffraction, corresponding to all the mortars (%)

	calcite $CaCO_3$ (PDF 05–0586)	dolomite $CaMg(CO_3)_2$ (PDF 84–1208)	Quartz SiO_2 (PDF 33–1161)	Feldspars phases	gypsum $CaSO_4{\cdot}2H_2O$ (PDF 33–0311)	portlandite (PDF 76–0571)	organic matter
ALCAZAR PALACE_ROMAN MORTARS (s. I–II)							
AP_R2i	25	–	70	< 5	–	–	–
AP_R3e	–	–	–	–	–	–	–
AP_R3i	25	–	70	< 5	–	–	–
AP_R10e	–	–	–	–	–	–	–
AP_R12i	25	–	70	< 5	–	–	–
AP_R12e	50	< 5	40	< 5	–	–	–
AP_R14i	25	–	70	< 5	–	–	–
AP_R14e	–	–	–	–	–	–	–
AP_R16i	25	–	70	< 5	–	–	–
AP_R16e	50	< 5	40	< 5	–	–	–
ALCAZAR PALACE_ARABIC MORTARS (s. XI)							
AP_A1i	30	–	65	< 5	–	–	–
AP_A1e	60	< 5	35	< 5	–	–	–
AP_A1bi	30	–	65	< 5	–	–	–
AP_A1be	–	–	–	–	–	–	–
AP_A2i	30	–	65	< 5	–	–	–
AP_A2e	60	< 5	35	< 5			
SHIPYARD_MEDIEVAL (s. XIII)							
SH_M2	70	< 5	30	–	–	–	–
SH_M5	75	< 5	25	–	–	–	–
SH_M28	75	< 5	25	–	–	–	–
SH_M30	55	< 5	40	< 5	–	–	–
ALCAZAR PALACE_MARCHENA DOOR (s. XV)							
AP_M1	70	< 5	25	–	–	–	–
AP_M2	70	–	25	< 5	–	–	–
AP_M3	65	–	25	< 5	5	–	–
AP_M4	70	–	25	< 5	–	–	–
AP_MD1*	–	55	30	–	10		–
AP_MD2*	55	–	15	–	25		–
SAN ISIDORO (s. XV–XVI)							
SI_M1	70	< 5	25	< 5	–	–	–
SI_M2	50	< 5	40	< 5	–	–	–
SI_M3	50	< 5	45	< 5	–	–	–
SI_M6	70	< 5	20	< 5	–	–	–
SI_M7	70	< 5	20	< 5	–	–	–
SI_M8	50	< 5	45	< 5	–	–	–
SI_M9	70	< 5	20	< 5	–	–	–
SI_M14	60	< 5	30	< 5	–	–	–
CITY HALL (s. XVI)							
CH_1*	50	–	25	–	–	–	6.34
CH_2*	35	< 5	10	–	20	–	10
CH_4*	50	–	20	< 5, mica	< 5	–	< 5
CH_5*	60	–	20	< 5	< 5	–	< 5
CH_6*	10	–	–	–	85	–	–

Table 2 (continued)

	calcite $CaCO_3$ (PDF 05–0586)	dolomite $CaMg(CO_3)_2$ (PDF 84–1208)	Quartz SiO_2 (PDF 33–1161)	Feldspars phases	gypsum $CaSO_4{\cdot}2H_2O$ (PDF 33–0311)	portlandite (PDF 76–0571)	organic matter
CH_8*	5	–	–	–	90	–	–
CH_9*	20	–	–	–	70	–	–
CH_10*	40	–	35	< 5, mica	< 5	–	< 5
CH_15*	95	< 5	–	–	< 5	–	–
CH_33*	95	< 5	–	–	< 5	–	–
CH_53*	65	< 5	–	–	35	–	2.29
CH_54*	50	–	–	–	50	–	> 2
CH_67*	55	< 5	–	–	35	–	11.65
CH_68*	–	–	–	–	–	–	–
CH_CM*	45	–	20	–	5	20	–
▲ *ROYAL ORDNANCE (s. XVIII)*							
RO_B	50	–	5	–	35	–	–
RO_C	60	–	5	–	30	–	–
RO_D	70	–	10	–	5	–	–
RO_F	55	–	40	–	< 5	–	–
RO_1Bl	–	–	–	–	–	–	–
RO_1Cl	–	–	–	–	–	–	–
RO_2	95	–	5	–	–	–	–
RO_3	55	–	10	–	35	–	–
RO_4Bl*	95	–	5	–	–	–	–
RO_4Cl*	85	–	10	–	–	–	–
▲ *SANTA MARIA_CUEVAS (s. XVIII)*							
SM_Ae	–	–	–	–	–	–	–
SM_Ai	60	< 5	25	–	–	–	–
SM_D	60	< 5	25	–	–	–	–
SM_I	60	< 5	25	–	–	–	–
SM_Ke	–	–	–	–	–	–	–
SM_Ki	60	< 5	25	–	–	–	–
SM_Le	35	–	20	–	40	–	–
SM_Li	60	< 5	25	–	–	–	–
SM_Me	–	–	–	–	–	–	–
SM_Mi	–	–	–	–	–	–	–
SM_N	–	–	–	–	–	–	–
▲ *EL SALVADOR (s. XVIII)*							
ES_CS1	–	–	–	–	–	–	–
ES_RSe	35	–	20	–	40	–	–
ES_RSi	–	–	–	–	–	–	–
▲ *SANTA ANGELA (s. XIX–XX)*							
SA_2	65	–	35	< 5	–	–	–
SA_6	55	40	–	< 5	–	< 5	–
SA_10	60	–	35	< 5	–	–	–
SA_12	50	–	30	< 5	–	20	–
SA_16*	55	–	15	–	–	30	–
SA_17*	5	55	30	–	–	5	–
SA_18*	35	50	5	–	–	10	–

* Restoration mortars

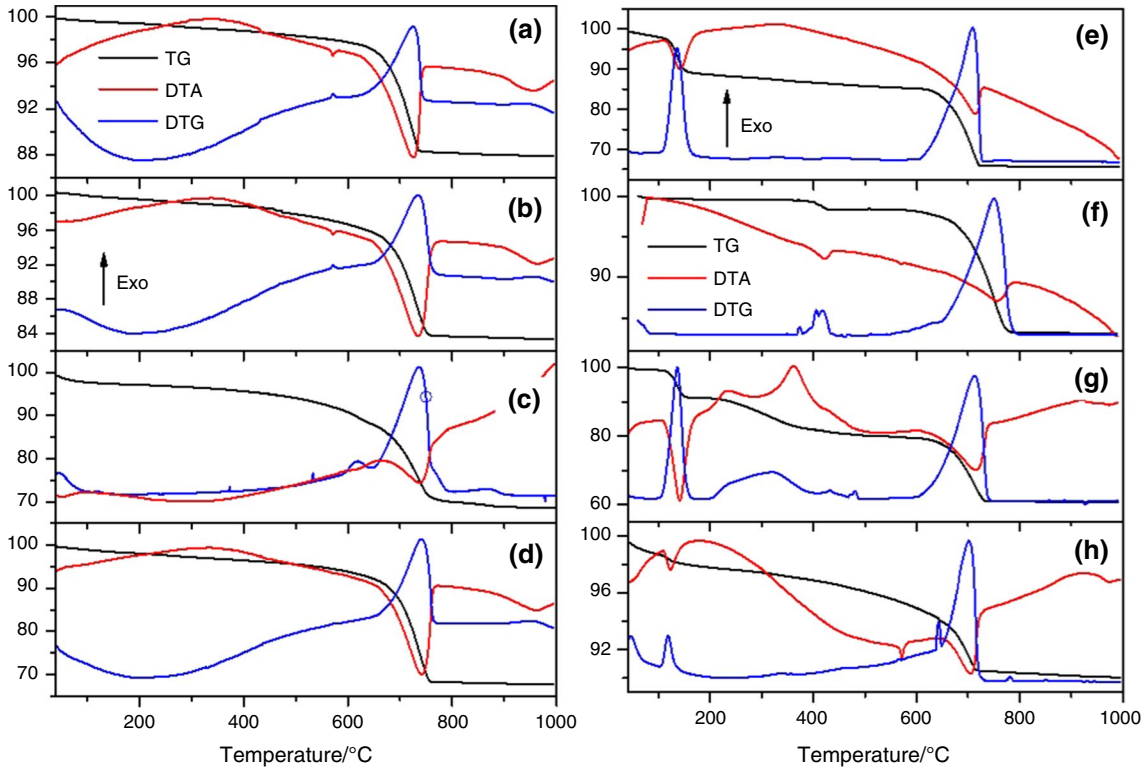

Fig. 4 Thermal curves (TG, DTG and DTA) of samples: **a** AP_R14i, **b** AP_A2i, **c** SH_M2, **d** SI_M8, **e** RO_B, **f** SA_17*, **g** CH_67*, **h** CH_CM*

quartz (samples SI_M1, SI_M6, SI_M7 and SI_M9) and another group with 50% of calcite (SI_M2, SI_M3, SI_M8 and SI_M14). Both mortar types corresponded to external and internal layers, respectively. EDX general analyses from the sample SI_M8 showed the presence of Si, Ca, Al and Fe (Fig. 7a).

Royal ordnance (eighteenth–twentieth centuries) (samples RO)

Although in Fig. 2 all samples from this artwork, except for samples RO_4Bl* and RO_4Cl* (considered as restoration mortars), are grouped in a unique zone, the carbonate percentages are very different for all RO samples (Table 1). The wall mortars were constituted by carbonates, sand aggregates and gypsum as observed by XRD (Table 2), while the resulting carbonate amounts were similar to those calculated by thermal analysis. The casting during manufacture of artillery materials was responsible of an important contamination producing the alteration of the mortars and the formation of gypsum in the surface (Table 2). The analyses by thermogravimetry also showed high contents of gypsum due to a high mass loss between 120 and 200 °C (Table 1). Both thermal curves (Fig. 4e) and XRD diffractogram (Fig. 5c) corresponding to sample RO_B (shown as example from this monument) clearly showed the presence of high amounts of calcite and gypsum ($CaSO_4{\cdot}2H_2O$, PDF 33–0311). The DTA curve showed two endothermic peaks at ca. 140 °C and ca. 710 °C attributed to release of water from the gypsum and release of carbon dioxide from carbonate, respectively. FTIR showed the characteristic vibrations of sulfate (gypsum) groups at 3540, 3406, 1115, 671 and 602 cm^{-1} and carbonate groups at 1796, 1405, 872 and 713 cm^{-1} (Fig. 6c). XRF analyses matched with the previous studies and Ca and S were detected in the sample (Table 3 and Supplementary Figure S1d). Some samples taken from wall surfaces RO_4Bl* and RO_4Cl* were made up almost exclusively of calcium carbonate as these zones were probably painted with lime in a restoration process.

Santa Maria Cuevas Monastery (fifteenth–eighteenth centuries) (samples SM)

Thermogravimetric data (Fig. 2 and Table 1) identified two groups of samples: the first one (samples SM_Ai, SM_D, SM_Ki, SM_Li, SM_Mi and SM_N) with high and the second one (samples SM_Ae, SM_Ke, SM_Le, SM_Me) with low concentrations of calcium carbonate. XRD with values of 60% (Table 2) corresponded to mortars used in wall manufacturing. Regarding the quantities of structural

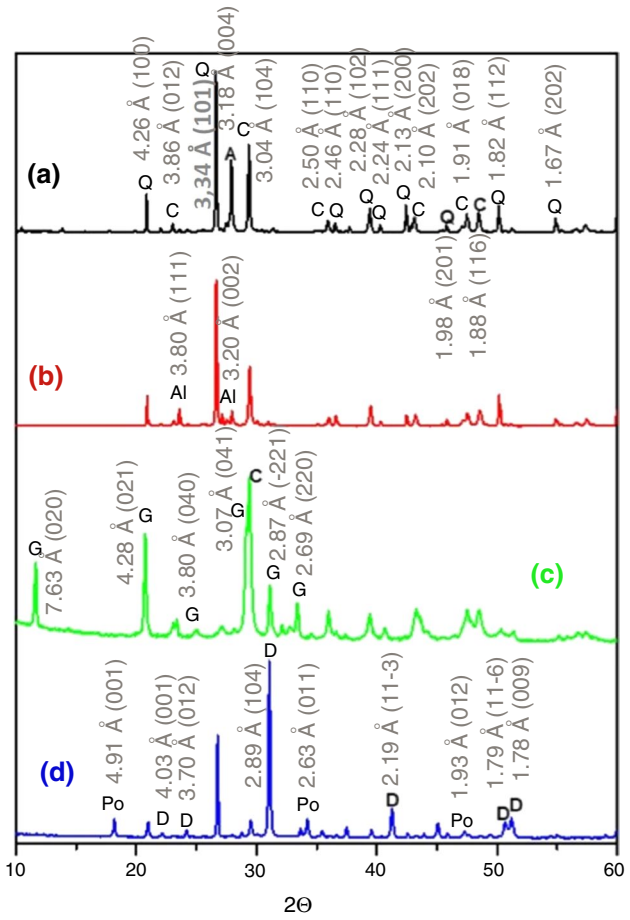

Fig. 5 XRD diffractograms corresponding to: **a** AP_R14i, **b** AP_A2i, **c** RO_B, **d** SA_17* [C = calcite, Q = quartz, A = anorthite, Al = albite, G = gypsum, D = dolomite, Po = portlandite]

water (Fig. 3), two different groups were also identified in line with the CO_2 mass losses. The low carbonate quantities for the second group were attributed to the fact that in the eighteenth century, the mortars were covered with gypsum stuccos with wall paintings. Moreover, the large mass losses observed in the temperature range between 120 and 200 °C for samples SM_Ae, SM_Ke, SM_Le and SM_Me (Table 1) could be attributed to the presence of large amounts of gypsum. In the case of external mortars, gypsum also was detected by XRD (Supplementary Figure S2). XRD (Table 2) shows that these mortars were constituted by sand aggregates (quartz) and binder (calcite).

El Salvador Church (eighteenth century) (samples ES)

The mortars studied from ES showed a high compositional heterogeneity (Table 1, Figs. 2 and 3). The differences could be assigned to the presence or absence of gypsum layer (stucco) in the samples. Two of the samples, ES_CS1 and ES_RSi, had high carbonate percentages, while for the other one (ES_RSe), the amount was much smaller. In this last sample, the percentage of gypsum was of 36.12% (Table 1). As an example of the experimental characterization, XRD diffractogram of the sample ES_RSe is shown in Supplementary Figure S3. Both the mortar and the mural paintings were made in the eighteenth century.

Santa Angela (nineteenth–twentieth centuries) (samples SA)

Two groups of mortars from the original construction period were discriminated in Santa Angela Convent monument (SA). One (SA_2, SA_6, SA_10 and SA_12) with high percentages of calcite (Tables 1 and 2) and quartz (Table 2). Gypsum was also detected in sample SA_12 by both XRD (Table 2) and thermogravimetry (Table 1). The other group consisted of three samples: SA_16*, SA_17* and SA_18*, which correspond to a recent intervention during the restoration of the wall: while the main component of sample SA_16* was calcium carbonate (Table 2), the other two (SA_17* and SA_18*) were constituted mainly of dolomite, as determined by DTA/TG in CO_2 atmosphere [33] and XRD (Table 2). Figure 4f shows the TG and DTA curves of the sample SA_17* which showed the presence of signals of water loss at ca. 440 °C attributed to the presence of portlandite ($Ca(OH)_2$) and of carbonates at ca. 770 °C by loss of CO_2. XRD diffractogram of the sample SA_17* is shown in Fig. 5d. Dolomite ($CaMg(CO_3)_2$, PDF 84–1208) was the main phase detected. XRF analyses matched with the previous studies and Mg and Ca were detected in the sample (Table 3 and Supplementary Figure S1e), indicating the presence of dolomite. Portland cement was detected in the three mortars. Portlandite ($Ca(OH)_2$, PDF 76–0571), attributed to Portland cement, was detected in the three mortars.

Table 3 XRF quantitative analyses (%) of some of the samples studied in this paper:

	MgO	Al_2O_3	SiO_2	P_2O_5	SO_3	Cl	K_2O	CaO	TiO_2	Cr_2O_3	MnO	Fe_2O_3	CuO
AP_R14i	1.25	8.79	37.27	0.00	0.59	0.26	1.17	47.14	0.44	0.05	0.07	2.62	0.34
AP_A2i	1.83	8.84	40.65	0.81	0.43	0.24	1.35	42.68	0.43	0.05	0.06	2.19	0.43
SH_M2	1.21	3.90	16.15	0.00	0.27	0.35	1.20	73.11	0.37	0.04	0.06	2.32	0.02
RO_B	0.34	0.11	1.44	1.83	22.96	0.41	0.32	71.52	0.00	0.04	0.02	0.90	0.13
SA_17*	21.54	1.88	13.75	0.00	0.43	0.00	0.52	59.84	0.19	0.04	0.08	1.72	0.02

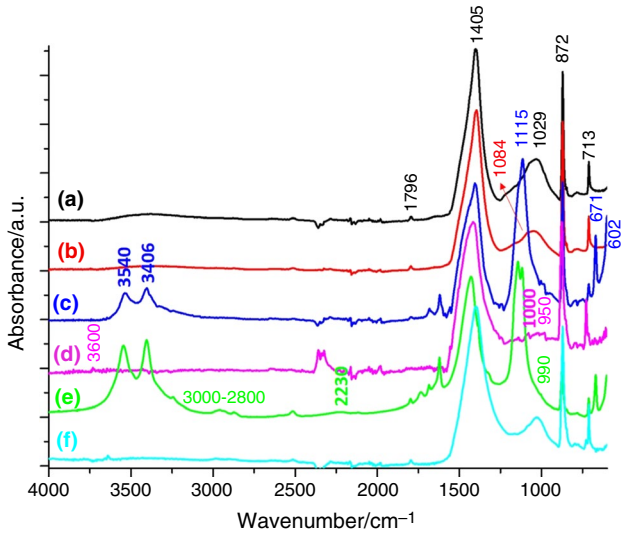

Fig. 6 FTIR spectra corresponding to: **a** SH_M2, **b** SI_M8, **c** RO_B, **d** SA_17*, **e** CH_67*, **f** CH_CM*

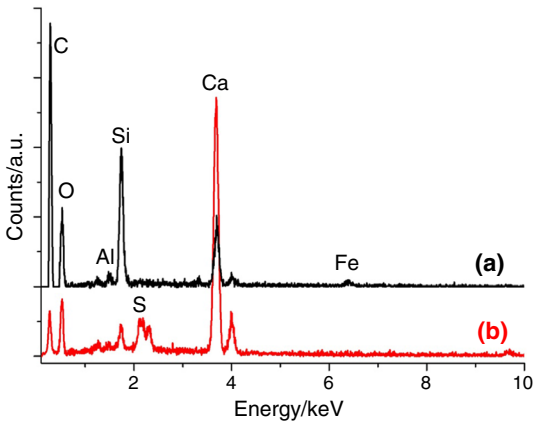

Fig. 7 EDX analyses of the samples: **a** SI_M8, **b** AP_MD2*

Phases of C_3S ($3CaO{\cdot}SiO_2$) and C_2S ($2CaO{\cdot}SiO_2$) were not found by XRD probably due to the lower powder diffraction, hydration and low percentages in the mixtures [34, 35]. Silicate calcium hydrates (CSH) are usually amorphous and they were not detected. Infrared spectrum of the sample SA17* showed signals attributable to cement compounds. In the case of the C_3S phase, Si–O stretching modes appeared at ca. 950 cm^{-1}. For C_2S phase, signals appeared at ca. 1000 cm^{-1}. Al–O stretching bands in C_3A ($3CaO{\cdot}Al_2O_3$) appeared in the range 900–750 cm^{-1} [36]. In addition, carbonates and hydroxylated compounds due to signal at ca. 3600 cm^{-1} also appeared (Fig. 6d). The TG curves showed mass losses attributed to the release of H_2O corresponding to $Ca(OH)_2$, especially for sample SA_18* (Table 1). It indicates that this mortar has been recently applied since $Ca(OH)_2$ is prone to carbonate with the atmospheric CO_2 and it does not last for long when exposed to air [37]. Regarding the distribution of the original samples (Fig. 2), the highest values of CO_2/H_2O were observed for SA mortars, mainly due to the low values of structural H_2O (Fig. 3) and the small quantity of clays present in the samples.

Mortars applied to building stones

Plasters were used to join stones, to cover the loss of original and restoration materials (inorganic and organic) employed to coat the buildings. Both Marchena Door (AP_M) and City Hall (CH) were constructed in the fifteenth and sixteenth centuries, respectively. Stones consisted of bioclastic fragments and fine sands [38–40]. During the restoration interventions, some of the stones, joining and lining mortars were substituted.

Marchena door (fifteenth century) (samples AP_MD)

It has undergone recent restoration processes. Two sample groups were clearly identified in Figs. 2 and 3. Original samples (AP_M1 and AP_M2) depicted values of CO_2/H_2O (Table 1) of ca. 6, closed to others from the fifteenth and sixteenth centuries (SI and SM). Restoration mortars (AP_MD1* and AP_MD2*) showed higher CO_2/H_2O values, with clearly minor amounts of clays (mass loss from 200 to 600 °C were very low, Fig. 3). The composition of AP_M1, AP_M2, AP_M3 and AP_M4 was mainly calcite and quartz (Table 2). Gypsum was also identified in the restoration samples by XRD (Table 2). EDX analyses corroborated the previous findings. Ca, Si and S were detected in the sample AP_MD2* (Fig. 7b).

Seville city hall (sixteenth century) (sample CH)

The high number of interventions and the use of different mortars were responsible for the heterogeneous distribution of points in Fig. 8 which includes the plot of structural H_2O vs CO_2 for the different samples studied from the City Hall.

Different types of samples were collected:

Samples CH_6*, CH_8* and CH_9* correspond to mortars used for joining stones, whose composition is mainly gypsum, as detected by DTA/TG (Table 1). XRD studies confirmed the presence of high amounts of gypsum, accompanied by anhydrite ($CaSO_4$, PDF 37–1496) and basanite ($CaSO_4{\cdot}0.5H_2O$, PDF 33–0310) (Table 2). The presence of gypsum indicated an inadequate restoration. In addition, calcite was also detected, mainly in sample CH_9*, probably as small rests of the calcite rock to which the mortar was attached as a surface plaster. Accordingly, the amount of carbonate mass loss in CH_6* and CH_8* was very low (Fig. 8).

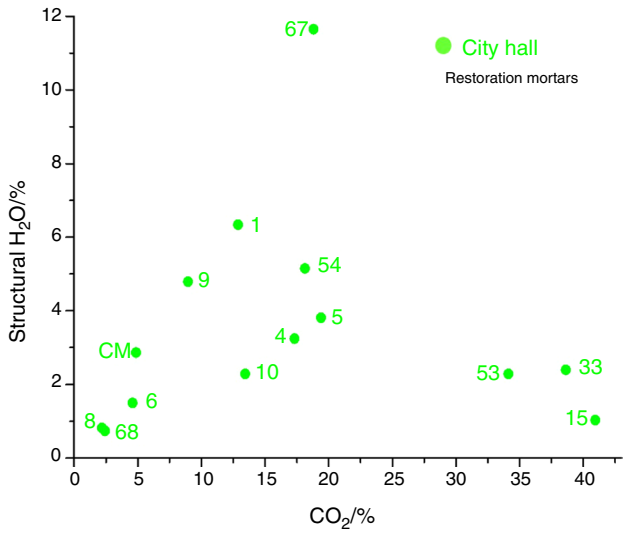

Fig. 8 Representation of % structural H_2O vs % CO_2 from mortars of the City Hall

The thermal and diffraction studies of samples CH_5* and CH_10* showed the presence of calcite and quartz (Tables 1 and 2), characteristic of lime mortars. In addition, gypsum appeared in low amounts and an exothermic peak, between 200 and 500 °C, in agreement with environmental contamination and/or deposition of combustion materials (very possible due to the presence of traffic around) after the application of this restoration mortar.

The DTA/TG analysis of the samples CH_15* and CH_33* showed a high mass loss from 600 °C (Fig. 8), attributed to the presence of calcite in high percentages (Table 1). There results were in line with the application of surface layers on original rocks in order to obtain color decoration.

The DTA/TG traces of sample CH_67* showed effects attributed to calcite and gypsum (Table 1). An important exothermic effect appeared and mass loss between 200 and 600 °C (Fig. 4g and 8), attributed to the presence of organic materials (acrylonitrile and others) [31]. The zone probably was altered due to sulfation process by environmental contamination and was added acrylonitrile to consolidate the material. Sample CH_1* showed similar characteristics of sample CH_67*, regarding the presence of organic restoration materials (Table 1). The infrared spectrum of this sample showed the presence of the gypsum and calcite vibrations, and also of organic compounds (Fig. 6e). Acrylonitrile was detected by infrared due to the presence of bands in the region 3000–2800 cm^{-1} which correspond to C–H stretching in alkene, CΞN signal at ca. 2230 cm^{-1}. At 990 cm^{-1} appeared the C=C signal (weak signals) [41].

Alumina cement was observed in the sample CH_68*, probably used in a recent restoration. The minor loss masses of CO_2 and structural water were observed for this sample (Fig. 8 and Table 1). A black crust of gypsum was observed in the surface of this monumental area as was detected by thermal analysis (Table 1). Alteration signs were also detected for samples CH_53* and CH_54* due to the presence of gypsum (by XRD) (Tables 1 and 2). Besides, it was detected a consolidant but in low amounts.

The composition of the sample CH_CM* was based on calcite, quartz, portlandite (showing the presence of Portland cement), dolomite and gypsum, which were detected by XRD (Table 2), employed in a restoration performed in the twentieth century. Figures 4h and 6f show the thermal curves and the infrared spectrum of this mortar sample.

The composition of the materials used in the restoration processes depended on the functions to be carried out. In this form, it was not the same to restore a lost mortar in a stone façade as it was to complete a piece of lost rock. It also affected the time in which they were applied [42]. For this reason, stone mortars and calcareous mortars, already described previously in this work, have also been used in the City Hall building. Inadequate processes were observed by the presence of organic materials or Portland cement. Nowadays, restoration mortars are constituted by mainly lime and sand compounds.

Comparison of mortars

Lining mortars

Roman (AP_R) (first–second centuries) and Arabic (AP_A) (eleventh century) mortars were very similar in composition and layer disposition: the ones used in inner parts could be identified as a real constructive mortar (25 and 30% calcite, respectively, by XRD, Tables 2 and 3, Figs. 5a, 5b and Supplementary Figures S1a and S1b). On top of these another surface layer, called stucco, with higher calcite content (50 and 60% of calcite in Roman and Arabic mortar, respectively). Both mortars were discovered in the Patio de Banderas of the Real Alcazar of Seville. The difference between mortars from these periods was a slightly higher concentration of carbonates in the Arabic mortars. In Figs. 2 and 3, only the inner part of the mortars was signed with dots. Arabic mortars showed higher structural water loss in the interval 200–600 °C than Roman ones (Figs. 3, 4a and 4b). Regarding the ratio CO_2/H_2O, the average values were higher for Roman (6.73) than for Arabic (5.18) due to the presence of an important mass loss due to structural water, probably due to the presence of clays or CSH phases.

Regarding the presence of hydraulic phases in ancient mortars, Collepardi stated that all the mortars employed for building before the advent of Portland cement can be defined as historic [43, 44]. In this sense, the mix of air-hardening lime and pozzolans and natural hydraulic lime have been

the most hydraulic binders found in ancient cultural heritage constructions, because hydraulic lime, formulated lime, natural cement, Portland cement and white cement are more recent in time (from the nineteenth century) [44]. By TG, the mass loss between 200 and 600 °C has been ascribed to the loss of structurally bound water from CSH and calcium aluminate hydrate (CAH) although the mass loss of organic substances is also found in this temperature range but showing exothermic effects (as aforementioned in this article); it is useful to find the correlation of CO_2 to the structurally bound water [44], as was made in this paper. XRD experiments could not distinguish the CSH phases because they are amorphous in hydraulic mortars.

The Shipyard medieval mortars (SH) (thirteenth century) used in later times than those previously mentioned had a different role in construction as joint for bricks. The composition was similar than the previously studied Roman and Arabic internal mortars. The samples presented higher carbonate percentage than the inner mortars and similar to the stuccos from the surface previously studied (AP_R and AP_A) (Figs. 2, Supplementary Figure S1c and 6a). In the TG curves, they presented the highest mass losses in the interval between 200 and 600 °C (structural H_2O) (Figs. 3 and 4c), due possibly to the presence of bricks rest in the studied mortars as visually observed in the monument. Values of ratio CO_2/H_2O ranged from 3.50 to 5.55, showing a higher hydraulic character than Roman or Arabic mortars. The determination of the mortar's type (pozzolanic, hydraulic or pure lime) is made by the ratio CO_2/H_2O. Most of the mortars studied are in the range 4–10, defined as hydraulic lime [7, 19]. In addition to this ratio, the presence of hydraulic phases was confirmed in almost all the cases by thermal analysis (mass loss between 200 and 600 °C and the absence of exothermic peaks due to organic compounds in this temperature range) and by infrared spectroscopy. Only AP_R12e could be considered as a true lime mortar because the value of ratio was higher than 10 (10.99).

This study matched with that from Sitzia [3] in which the use of brick-rubble and pozzolanic materials in Medieval times was higher than in Roman period for mortars from Cagliari, Italy. Also, our results are in line with mortars from Florence riverbanks from the thirteenth century, which consists of natural hydraulic lime binder. The hydraulic characteristics allow hardening and preservation under high humidity conditions [17]. Usually mortars binders employed in medieval times were found to be made of lime, except in some cases in which magnesian mortars have been described [16]. In Sevillian mortars, structural water amount (coming from clays and pozzolanic components) was higher for Medieval (SH) than Roman (AP_R) or Arabic (AP_A) mortars (Fig. 3, Table 1). This result is contrary to others described in the literature [4–6] in which a gradual decline in the quality of the mortars was observed for Medieval times. In this sense, a recent study of mortars from Transylvania, dated from the first century BC until Medieval times only showed the presence of true lime mortars because the ratio was higher than 28 [7] and also in Gothic (thirteenth–fifteenth centuries) mortars from Slovenia [45].

Construction (inner) mortars from the fifteenth–eighteenth centuries (SI, RO, SM and ES) were found in a very similar zone of Figs. 2, 3, 5c, S2, S3, Supplementary Figure S1d, 6b, 6c and 7a. All the values were delimited between mass losses of CO_2 between 18.55% (RO_F) and 31.48% (ES_RSi) and structural H_2O mass losses between 2.95% (RO_C) and 5.98% (ES_RSi) (Fig. 3, 4d and 4e). In comparison with the more ancient mortars (AP_R, AP_A, SH), the ratio CO_2/H_2O was very similar to those from the fifteenth–eighteenth centuries. However, the amount of loss assigned to structural water was higher for the more recent (SI, RO, SM and ES) (Fig. 3). In the case of SM and ES, gypsum stuccoes were laid on the inner mortars in order to decorate the paintings. Recently, six mural paintings from the medieval university of Fez were examined, showing the presence of gypsum and calcite layers [46]. In the case of the RO, the presence of gypsum was assigned to contamination. In Mudejar samples from Zaragoza (Spain) binder consisted mainly of gypsum to which lime was added although in low proportion [47]. The ground layer of the high-relief stuccoes from different Central European artworks dated between the sixteenth and eighteenth centuries was made with lime, gypsum and unselected sand [48], similarly to those described in this work.

For SI, two groups of mortars, inner and surface ones (supporting fresco paintings), were observed, similar to those from Roman (AP_R) and Arabic (AP_A). The highest structural water losses for the more modern mortars (SI, RO, SM and ES) coincided with some other publications which indicated that after the fourteenth century, Vitruvius books were reread [49]. Hydraulic lime was discovered at the eighteenth century and the constructive technology was notably improved [49].

The mortars from Santa Angela (SA) convent showed high percentages of carbonates, being the ratio CO_2/H_2O very high, from 10.60 to 19.12 in three (SA_2, SA_6 and SA_10) of the four original mortars (Fig. 2), that were considered as lime mortars in a comparative mode.

Regarding the restoration mortars, applied later than the original construction mortars, two of them are from RO (RO_4Bl* and RO_4Cl*) and three from SA (SA_16*, SA_17* and SA_18*) (Figs. 4f, 5d and 6d). In the case of the monument from the eighteenth century (RO), lime mortars were applied while Portland cements were used from the convent of the nineteenth century. Only one of the original mortars (SA_12) showed 20% of Portland cement (Table 3).

Mortars applied to building stones

The mortars mainly applied to join stones from Marchena Door and Seville City Hall were constituted by carbonates and sand aggregates, similarly to others studied in this manuscript. The most complex and interesting studies on mortars applied for conservation and restoration were those carried out on stones monuments such as Marchena Door (AP_M) and Seville City Hall (CH), mainly the latter on its main façade toward *Plaza San Francisco*, which was where its construction began in the sixteenth century. Due to the industry, traffic, climate changes, the tastes of the authorities, political influences, economic interests, etc., the building has undergone many interventions for its maintenance although some restoration processes were not appropriated. At the beginning, they were done with the knowledge of the epoch, which is not the current one, or by non-specialist staff.

The mortars used in Marchena Door (AP_M and AP_MD) and City Hall of Seville (CH) had a high heterogeneity in composition. Although calcite and aggregates (silica-calcareous) were detected in all the samples, gypsum was the main component in some of the City Hall mortars (Table 2). The mortars applied in the restoration of Marchena Door were also applied in the restoration of Santa Angela Convent.

In addition, the thermal study carried out in this work has allowed the characterization of other multiple materials used in the various interventions carried out on the Seville City Hall building (Table 1), as was mentioned before: plaster, mixtures of calcium carbonate or dolomite with Portland cement, portlandite $Ca(OH)_2$, alumina cement, consolidate (acrylic resin). This variety of composition was responsible for the heterogeneity of points shown in Figs. 4g, h, 6e, f and 8. Depending on the period in which the restoration was performed, materials were different: gypsum was found in the filling of the stones from the first epochs (CH_6*, CH_8* and CH_9*). More recently, Portland cement mortars began to be manufactured and applied as restoration or filling mortars (CH_CM*), and also organic polymers were used and found (CH_1*, CH_2* and CH_67*). Similar composition in other mortar samples was previously described by [20].

Lime mortars were considered as the constructive elements of architectural heritage until the end of the eighteenth century [50] when Portland and other types of cements were introduced in order to improve the strength of the mortars and the adhesion to bricks and stones [50]. However, the introduction of Portland cement in restoration processes caused damages to the original materials due to the salts crystallization frequently occurring, as mentioned in a recent study from a Serbian wall fortification of the fourteenth century [50]. Also, different calcium aluminate and aluminoferrite phases were recently identified in three building in Switzerland at the final of the nineteenth century [51]. Polymers and organic compounds have been also been found as reinforcing elements [52]. There are similarities between all these recent studies and our findings in the mortars studied from the Seville City Hall.

Comparison of maximum temperature obtained by DTG of carbonate thermal decomposition

The thermal decomposition of carbonates of the mortars studied in this manuscript occurred in a large temperature range. It is very well known that thermal decomposition of carbonates is function of the history of the materials, crystallinity and fragmentation of materials [53]. Figure 9 shows the DTG curves of a selection of some of the studied samples in this manuscript.

The stone materials used to build the City Hall (CH) and Marchena Door (AP_M and AP_MD) are carbonate-based compounds of bioclastic fragments (polycrystalline aggregates) and fine sand. The DTG of the carbonate of the mortars applied to stones (Fig. 9a) showed the maximum decomposition temperature about 800 °C in agreement with polycrystalline carbonate materials. Results similar were obtained for mortars used in recent intervention on the buildings as micro-mortar for injection, consolidation or reconstruction material constituted by marble powder with high purity as those of CH53*.

Mortars recently used for restoration of walls in Santa Angela de la Cruz convent (SA_16*, SA_17* and SA_18*) were constituted by carbonates (calcite + dolomite or only calcite) together with quartz and portlandite (Tables 2, 3 and Supplementary Fig. S1e). The DTG curves of these samples showed high carbonate decomposition temperatures (Fig. 9b), but a little lower than the mortars used in stone building (Fig. 9a) (maximum temperature at ca. 770 °C). The DTG curves of the samples containing dolomite showed two peaks when heating in CO_2 atmosphere, attributed to

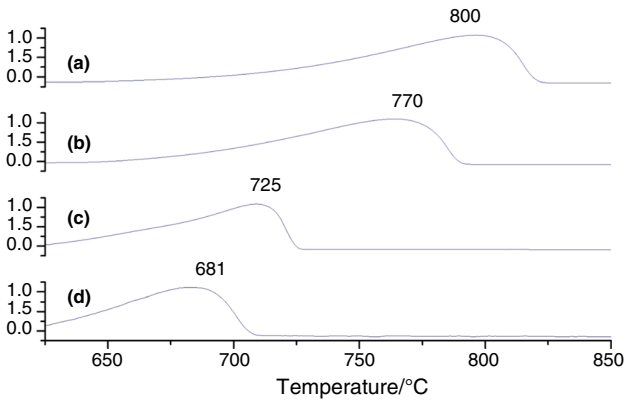

Fig. 9 DTG curves corresponding to mortars from: **a** CH, **b** SA, **c** AP_R, **d** SI

the Mg and Ca compounds present in this carbonate [35]. Original samples used in this building (constituted mainly by calcite and quartz) (Table 2) showed maxima temperatures in the DTG curves similar than the previous studied samples (Fig. 9b). Portlandite was not found due to the carbonation processes [42]. The use of dolomitic lime mixed with gypsum was referred for Bartz et al. in the Baroque Post-Cistercian abbey in Lubiaz in Poland [54].

The inner Roman and Arabic mortars (AP_R and AP_A) showed DTG curves with similar values of carbonate decomposition temperatures between 715 and 735 °C (Fig. 9c) for all the studied mortars. The values were lower than the previous studied mortars. Two samples of the medieval Shipyards (SH_M2 and SH_M5) showed similar values than those of the AP_R and AP_A.

Some mortars of the San Isidoro Monastery (SI) showed the lowest carbonate decomposition temperatures of the DTG curves, at about 681 °C (Fig. 9d). This thermal decomposition was attributed to the carbonates present in the external layer of the fresco used for the ornamentation of the walls (produced by carbonation of lime). Similar results were obtained in the external layers of Roman and Arabic mortars from the Alcazar Palace (AP_R and AP_A) and also from other buildings such as Santa Maria de las Cuevas Monastery (SM) and El Salvador Church (ES). The decrease in decomposition temperature of carbonates in these samples might be due either to the presence of compounds that favor decomposition, especially salts. In the mortars with high percentage of gypsum added or produced by contamination and organic compounds added as pollutants or consolidants studied in this manuscript produced a decrease in the maximum temperature of DTG.

The mortars of the Royal Ordnance (RO) showed a wide temperature decomposition range (721, 727, 739, 746, 752, 753 and 756 °C) due to the different alteration processes of the walls and the restoration carried out on them.

Conclusions

The following research has been focused on the composition and production technology of mortars used in different historical periods in Seville, from Romans to present times, including Arabic, Mudejar and different Cristian periods. The compositions of the Roman (AP_R) and Arabic (AP_A) mortars were very similar, although with different amounts of clays. Moreover, medieval Shipyard mortars (SH) also showed similar compositions to the Roman and Arabic ones but with smaller CO_2/H_2O ratios due to the presence of brick traces. Regarding the samples from the fifteenth–eighteenth centuries (San Isidoro Monastery, SI, Royal Ordnance Factory of Seville, RO, Santa María de las Cuevas, SM and El Salvador Church, ES), the CO_2/H_2O ratios were similar to more ancient ones (AP_R, AP_A and SH) but with larger amounts of structural water. Most mortars can be considered as hydraulic, with CO_2/H_2O ratios between 4 and 10. Moreover, the hydraulic phases, from which structurally bound water was released, could be identified in some samples by either FTIR (SH_M2, SI_M8, SA_17* and CH_CM*, Fig. 6) or XRD (SA_17*, Fig. 5).

In some samples, such as those from San Isidoro Monastery (SI) and Santa María (SM) de las Cuevas, differences in terms of the presence of gypsum and the painting techniques are quite evident. Moreover, the industrial activities carried out in some of the investigated buildings affected the composition of the mortars, as is the case of the samples of the Royal Ordnance Factory of Seville (RO). In the case of the Santa Angela convent (SA), all mortars are of modern manufacture.

In general, it was found for Sevillian mortars that the older the building the lower the amount of structural water. Thus, Roman (AP_R) or Arabic (AP_A) mortars have smaller amount of structural water than Medieval ones (SH), while the latter ones have smaller amount than more modern ones (SI, RO, SM and ES).

In the case of studied stone buildings, such as the Marchena Door or the City hall, mortars are quite heterogeneous due to the different restorations performed along several centuries. Thus, original mortars consist of sand aggregates (quartz) and binder (lime). For subsequent interventions, gypsum was used in the first restorations and Portland and/or others (lime + calcite aggregates, dolomite lime + siliceous aggregates, lime + Portland cement, etc.) and organic polymers in the most recent restorations. This variety of composition was responsible for the broad dispersions of CO_2/H_2O ratios.

Supplementary Information The online version contains supplementary material available at https://doi.org/10.1007/s10973-023-12313-y.

Author contributions J.L. Perez-Rodriguez and A. Duran were involved in conceptualization; J.L. Perez-Rodriguez and A. Duran helped in methodology; J.L. Perez-Rodriguez, L.A. Perez-Maqueda, M.L. Franquelo and A. Duran contributed to formal analysis and investigation; J.L. Perez-Rodriguez and A. Duran were involved in writing—original draft preparation; J.L. Perez-Rodriguez and A. Duran helped in writing—review and editing; J.L. Perez-Rodriguez contributed to funding acquisition; J.L. Perez-Rodriguez and A. Duran were involved in resources; J.L. Perez-Rodriguez and A. Duran helped in supervision.

Funding Open Access funding provided thanks to the CRUE-CSIC agreement with Springer Nature.

References

1. Vitruvius, in Morgan, M. H., editor. De architectura libri decem, II (materials) and VII (finishes and colours). Whitefish: Kessinger Publishing; 2005.
2. Pliny the Elder. Natural history. Paris: Les belles lettres; 1985.
3. Sitzia F. The San Saturnino Basilica (Cagliari, Italy): An up-close investigation about the archaeological stratigraphy of mortars from the Roman to the Middle Ages. Heritage. 2021;4(3):1836–53.
4. Artioli G, Secco M, Addis A. The vitruvian legacy: Mortars and binders before and after the Roman world. Eur Mineral. 2019. https://doi.org/10.1180/EMU-notes.20.4.
5. Moropoulou A, Bakolas A, Bisbikou K. Investigation of the technology of historic mortars. J Cult Herit. 2000;1(1):45–58.
6. Furlan V, Bissegger P. (1975) Les Mortiers Anciens: Historie et Essais D'analyse Scientifiques ancient Mortars: History and Approach to Scientific Examination, Zeitschrift Schweizerische Archâeologie Und Kunstgeschichte, Rev; Suisse d'art d'archaeologie: Zurich, Switzerland
7. Vlase G, Vlase D, Ferencz IV, Sfirloaga P, Micle D, Menea F, Vlase T. Comparative thermal and hyphenated analysis of different mortars samples from Deva region. J Thermal Anal Calorimet. 2022;147:5365–76.
8. Garofano I, Perez-Rodriguez JL, Robador MD, Duran A. An innovative combination of non-invasive UV-Visible-FORS, XRD and XRF techniques to study Roman wall paintings from Seville, Spain. J Cultural Heritage. 2016;22:1028–39.
9. Robador MD, de Viguerie L, Perez-Rodriguez JL, Rousseliere H, Walter P, Castaing J. The structure and chemical composition of wall paintings from Islamic and Christian times in the Seville Alcazar. Archaeometry. 2016;58(2):255–70.
10. Garofano I, Robador MD, Duran A. Materials characterization of Roman and Arabic mortars and stuccoes from the Patio de Banderas in the Real Alcazar of Seville (Spain). Archaeometry. 2014;56:541–61.
11. Duran A, Perez-Rodriguez JL, Jimenez de Haro MC, Franquelo ML, Robador MD. Analytical study of Roman and Arabic wall paintings in the Patio de Banderas of Reales Alcazares' Palace using non-destructive XRD/XRF and complementary techniques. J Archaeol Sci. 2011;38:2366–77.
12. Garofano I, Duran A, Perez-Rodriguez JL, Robador MD. Natural earth pigments from Roman and Arabic wall paintings revealed by spectroscopic techniques. Spectrosc Lett. 2011;44:560–5.
13. Cowper AD. Lime and lime mortars. UK: Routledge; 2017.
14. Elsen J, Balen K, Mertens G. Hydraulicity in historic lime mortars: a review. Historic Mortars. 2012;2012:125–39.
15. Jackson MD, Ciancio Rossetto P, Kosso CK, Buonfiglio M, Marra F. Building materials of the theatre of Marcellus, Rome. Archaeometry. 2011;53(4):728–42.
16. Milanesio E, Storta E, Gambino F, Appolonia L, Borghi A, Glarey A. Petrographic characterization of historic mortar as a tool in archaeologic study: examples from two medieval castles of Aosta Valley, Northwest Italy. J Archaeol Sci Rep. 2022;46:103719.
17. Calandra S, Salvatici T, Centauro I, Cantisani E, Garzonio CA. The mortars of Florence riverbanks: raw materials and technologies of Lungarni historical masonry. Appl Sci. 2022;15:5200.
18. Andrejkovicova S, Maljaee H, Rocha D, Rocha F, Soares MR, Velosa A. Mortars for conservation of late 19th and early 20th century buildings—combination of natural cements with air lime. Materials. 2022;15:3704.
19. Duran A, Robador MD, Jimenez de Haro MC, Ramirez-Valle V. Study by thermal análisis of mortars belonging to wall paintings corresponding to some historical buildings of Sevillian art. J Therm Anal Calorim. 2008;92:353–9.
20. Robador MD, Arroyo F, Perez-Rodriguez JL. Study and Restoration of the Seville City Hall façade. Constr Build Mater. 2014;53:370–80.
21. Robador MD, Perez-Rodriguez JL, Duran A. Hydraulic structures of the Roman Mithraeum house in Augusta emerita Spain. J Archaeological Sci. 2010;37:2426–32.
22. Bakolas A, Biscontin G, Moropoulou A, Zendri E. (1996) Dal sito archeologico all'archeologia del costruito, Proc. Scienza e Beni Culturali XII, Bressanone, pp. 613–623
23. Chiari G, Santarelli ML, Torraca G. Materiali e Strutture. 1992;3:111–37.
24. Bakolas A, Biscontin G, Contardi V, Franceschi E, Moropoulou A, Palazzi D, Zendri E. Thermoanalytical research on traditional mortars in Venice. Thermochim Acta. 1995;270:817–28.
25. Bakolas A, Biscontin G, Moropoulou A, Zendri E. Characterization of structural byzantine mortars by thermogravimetric analysis. Thermochim Acta. 1998;321:151–60.
26. Perez-Rodriguez JL, Franquelo ML, Duran A. TG, DTA and X-ray thermodiffraction study of wall paintings from the fifteenth century. J Therm Anal Calorim. 2021;143:3257–65.
27. Duran A, Perez-Rodriguez JL. Revealing Andalusian wall paintings from the 15th century by mainly using infrared spectroscopy and colorimetry. Vib Spectrosc. 2020;111:103153.
28. Robador MD, Mancera I, Perez-Maqueda R, Albardonedo A. Study of the wall paintings of the Cenador del Leon in the Real Alcazar of Seville. IOP Conf Series: Mater Sci Eng. 2017;245:082003.
29. Robador MD, Albardonedo A, Perez-Rodriguez JL. Evolution study of colours throughout the history of façades of the Royal Ordnance Factory of Seville. Proc Eng. 2016;161:1678–82.
30. Robador MD, Albardonedo A, Perez-Rodriguez JL. Colours found during restoration of the Seville City Hall façade. Proc Eng. 2016;161:1673–7.
31. Franquelo ML, Robador MD, Perez-Rodriguez JL. Study of coatings by thermal análisis in a monument built with calcarenite. J Therm Anal Calorim. 2015;121:195–201.
32. Robador MD. Restauración de la Puerta de Marchena del Real Alcázar de Sevilla: respeto a la huella del tiempo. Apuntes del Alcázar de Sevilla. 2014;15:61–86.
33. Perez-Rodriguez JL, Duran A, Perez-Maqueda LA. Thermal study of unaltered and altered dolomitic rock samples from ancient monuments: the case of Villarcayo de Merindad de Castilla la Vieja (Burgos, Spain). J Thermal Anal Calorim. 2011;104(2):467–74.
34. Giraldo MA, Tobón JI. Mineralogical evolution of Portland cement during hydration process. Dyna Rev Fac Nac Minas. 2006;73:1–9.
35. Trezza MA, Scian AN. Technical contribution DTA/TG and FT-IR spectroscopy to the study of carbonation of the cement matrix. Afinidad. 2013;70(562):112–7.
36. Hughes TL, Methven CM, Jones TGJ, Pelham SE, Fletcher P, Hall C. Determining cement composition by Fourier Transform Infrared Spectroscopy. Adv Cem Based Mater. 1995;2:91–104.
37. Blanco MT, Puertas F, Vazquez T, de la Fuente A. The most suitable techniques and methods to identify high alumina cement and based Portland cement in concrete. Mater Constr. 1992;42(228):51–64.
38. Guerrero Montes MA. Diagnóstico del estado de alteración de la piedra del palacio consistorial de Sevilla. Causas y mecanismos: Universidad de Sevilla; 1990.

39. Alcalde M, Martín A. Morfología macroscópica de alteración acelerada de algunos materiales pétreos de monumentos de Andalucía. Mater Constr. 1990;40:5–37.
40. Lazzara G, Fakhrulin R. Nanotechnologies and Nanomaterials for Diagnostic Conservation and Restoration of Cultural Heritage. USA: Elsevier; 2018.
41. Radhi MM, Tan WT, Rahman MZB, Kassim AB. Synthesis and characterization of grafted acrylonitrile on polyestirene modified with activated carbon using gamma-irradiation. Sci Res Essays. 2012;7:790–5.
42. Stepkowska ET, Aviles MA, Blanes JM, Perez-Rodriguez JL. Gradual transformation of $Ca(OH)_2$ into $CaCO_3$ on cement hydration: XRD study. J Therm Anal Calorim. 2007;87(1):189–98.
43. Collepardi M. Degradation and restoration of masonry walls of historical buildings. Mater Struct. 1990;23:81–102.
44. Arizzi A, Cultrone G. Mortars and plasters—how to characterise hydraulic mortars. Archaeol Ahthropol Sci. 2021;13:144.
45. Kriznar A, Höfler J, Ruiz-Conde A, Sanchez-Soto PJ. Caracterización arqueométrica de pigmentos y soportes procedentes de pinturas murales góticas. Boletín de la Sociedad Española de Cerámica y Vidrio. 2007;46(2):76–87.
46. Fikri I, El Amraoui M, Haddad M, Ettahiri AS, Falgueres C, Bellot-Gurlet L, Lamhasni T, Ait Lyazidi S, Bejjit L. Raman and ATR-FTIR analyses of medieval wall paintings from al-Qarawqiyyin in Fez (Morocco). Spectrochimica Acta Part A. 2022;280:121557.
47. Igea J, Lapuente P, Martínez-Ramírez S, Blanco-Varela MT. Characterization of Mudejar mortars from St. Gil Abbot church (Zaragoza, Spain): investigation of the manufacturing technology of ancient gypsum mortars. Mater Constr. 2012;62(308):515–29.
48. Caroselli M, Valek J, Zapletalova J, Felici A, Frankeova D, Kozlovcev P, Nicoli G, Jean G. Study of materials and technique of late Baroque stucco decorations: Baldasarre Fontana from Ticino to Czechia. Heritage. 2021;4(3):1737–53.
49. Amoroso G. Tratatto di Scienza della Conservazione dei Monumenti. Italy: Alinea; 2002.
50. Vasovic D, Terzovic J, Kontic A, Okrajnov-Bajic R, Sekularac N. The influence of water/binder ratio on the mechanical properties of lime-based mortars with white Portland cement. Crystals. 2021;11:958.
51. Dariz P, Neubauer J, Goetz-Neunhoeffer F, Schmid T. Calcium aluminates in clinker remnants as marker phases for various types of 19th-century cement studied by Raman microspectroscopy. Eur J Mineral. 2016;28:907–14.
52. Alves RAA, Strecker K, Pereira RBD, Panzera TH. Mixture design applied to the development of composites for steatite historical monuments restoration. J Cult Herit. 2020;45:152–9.
53. Duran A, Perez-Maqueda LA, Poyato J, Perez-Rodriguez JL. A thermal study approach to Roman age wall painting mortars. J Thermal Anal Calorim. 2010;99:803–9.
54. Bartz W, Kierczak J, Gasior M, Zboinska K. Analytical overview of different Baroque plastering techniques applied in the post-Cistercian abbey in Lubiaz (South-Western Poland). J Cult Herit. 2017;28:37–47.